

# On-Line Detection of Abnormal Cyclone Performance using Particle Size Tracking (PST) Technology

Jaime Sepulveda<sup>1</sup>, Robert Maron<sup>2\*</sup>, Mauricio Estrada<sup>3</sup>, Rodrigo Bruna<sup>3</sup>

1. *J-Consultants Ltd., Chile*
2. *CiDRA Minerals Processing Inc, USA*
3. *SGS, Chile*

## ABSTRACT

The recent emergence of reliable, real-time direct particle size measurement on individual hydrocyclones has overcome a long-standing, underserved need in mineral processing. It is well known that good control of the final particle size produced by the grinding-classification circuit is a critical measurement. Its poor control can have many adverse effects: e.g. lower throughput, poor flotation performance, and ultimately, lower net metal production.

In order to obtain full benefits of the commercially available CiDRA CYCLONetrac Particle Size Tracking (PST) technology, particle size measurements of each individual cyclone overflow stream must be incorporated into the corresponding Expert Control Strategy, to take advantage of PST's unique capability to detect on-line abnormal cyclone performance (e.g. excessively coarse product size that can lead to apex roping or plugging) of any specific cyclone at any point in time during line operation. In this context, PST allows for the implementation of selective open/close protocols for each of the cyclones around the whole classifier cluster.

In this paper the authors propose examples of advanced process control strategies that incorporate the particle size signals generated from each hydrocyclone, as could be applied to a typical SAG/Ball milling line. Proper implementation of the proposed control strategy is expected to deliver significantly lower variability of the final product size fed to downstream flotation, and thus, enable more closely approaching downstream process barriers. This is a particularly important goal given the emerging trend toward coarse particle recovery which requires grinding coarser while staying within the existing limits of the process and equipment.

**\*Corresponding author:** CiDRA Minerals Processing, Inc., Managing Director, Latin America, 55 Barnes Park North, Wallingford, CT, USA 06492. Email: [rmaron@cidra.com](mailto:rmaron@cidra.com)

## INTRODUCTION

The many challenges facing the mining industry, such as water shortages, rising energy cost, declining grades and harder ores, are driving innovation in many areas, a significant one being coarsening the final product size and recovering the resulting coarser particles. Coarser grinding can increase throughput and reduce water and specific energy consumption; however, it requires changes in the operation of the milling circuit. As throughput increases and existing process barriers are more closely approached, it becomes increasingly important to be able to continuously measure and control the final product size to avoid process upsets and losses in flotation recovery.

To assess the attainable benefits of grinding coarser, the authors developed a methodology using historical plant data in terms of the resulting increase in Net Metal Production (Maron et.al 2017) and have also explored some of the challenges and enabling technologies related to coarser grinding (Maron et.al. 2019). This work explores in depth the challenge of operating cyclones closer to their operating limits to produce higher throughput at a coarser final product size.

The hydrocyclone classifiers normally used in closed circuit grinding operations with conventional ball mills play a critical role in determining the final product size. Hydrocyclones are typically configured in groups or clusters of up to a dozen or more, fed radially from a central slurry distributor. When all operating cyclones are classifying properly, their overflow streams (the final ground product typically fed to the downstream flotation stage) have approximately equal flowrates and ideally identical particle size distributions (PSD). However, when one cyclone of the cluster begins to operate abnormally, such as classifying much coarser than the others due to partial/total blockage or plugging of its lower apex outlet, its overflow stream flowrate increases significantly, and its PSD becomes much coarser compared to the other normally operating cyclones.

This coarsening of the overflow stream PSD of the apex-plugged cyclone happens because as the apex approaches the fully plugged condition, the flow through the plugged apex decreases to zero, and the overflow stream becomes similar to the feed stream. Therefore, the overflow PSD must necessarily approach that of the feed stream PSD. This results in circulating load particles – still too coarse because they have not yet been ground to the desired P80 target – being directed to the overflow, which results in a decrease in recovery.

Figure 1 illustrates an actual industrial scale example where, at some point in time, Cyclone 9 went into an apex partially or fully plugged condition producing an overflow stream significantly coarser than the other cyclones, which then began to produce a somewhat finer overflow product. Although not shown in the graph, the PSD of the combined overflow stream of the entire cyclone cluster likely became slightly coarser as will be shown later through simulation. Therefore, if only the combined overflow stream were to be monitored – and not every cyclone individually – then this could have been misinterpreted as being caused by an increase in hardness of the feed ore. Thus, the likely action of operators or the control system would have been to simply reduce the fresh tonnage to the grinding line, with all its consequential circuit performance losses. Important to note that this condition was maintained for at least 1 hour without any corrective control actions.

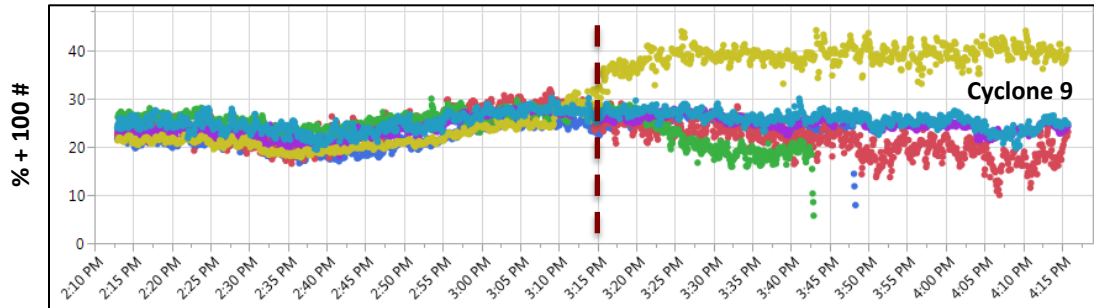


**Figure 1.** Multiple PST particle size signals (% + 100#) on hydrocyclone overflow streams operating normally with similar overflow PSD's, when suddenly Cyclone 9 becomes very coarse affecting all other cyclones in the same cluster.

These sorts of mostly unnoticed process contingencies are known to occur with considerable frequency in all grinding/classification operations. Therefore, there is a need to find and implement effective process control solutions for the prompt detection and correction of abnormally performing cyclones by remotely commanding their immediate replacement with other idle cyclones in the cluster until proper maintenance on the abnormal cyclone is performed. A novel acoustic impact-based technology developed by CiDRA Minerals Processing allows for real-time tracking of the particle size in the overflow stream of each individual cyclone in the cluster (see Figure 2). Known as CYCLONetrac Particle Size Tracking (PST), it is being used in many large-scale operations throughout the world, delivering increased throughput and recovery with near 100% availability and minimal maintenance. It overcomes the limitations of previously available 'near-line' technologies, related to serious operational difficulties associated with slurry sampling and transportation to the remote measurement instrumentation. When properly incorporated into an Expert Process Control strategy, PST's reliable real-time particle size measurement on every hydrocyclone overflow stream enables operators to coarsen the product size and more confidently approach the always existing and unavoidable downstream process limits. Further, as proposed in the current publication, PST technology allows for the detection and prompt correction of abnormally performing cyclones by commanding their prompt replacement by other idle cyclones in the cluster until proper maintenance on the abnormal cyclone is performed.

## IMPACT-BASED REAL-TIME HYDROCYCLONE PARTICLE SIZE MEASUREMENT

PST technology implementation is centered upon a sensor probe that is inserted into the overflow slurry stream via a two-inch (50 mm) hole in the overflow pipe. Particles within the slurry stream impact the surface of the probe generating traveling stress waves within the probe. A sensor converts these traveling stress waves into an electrical signal, and proprietary signal processing techniques convert these signals into a particle size measurement that is output every four seconds. The sensor is constantly in contact with many particles in the slurry stream, thus obtaining information from orders of magnitude more particles than traditional sample-based technologies. Also, because of the location of the sensor downstream of the hydrocyclone and the presence of an air core at that point, the sensor produces no change in the back pressure seen by the hydrocyclone and thus does not affect hydrocyclone performance. Due to abrasive wear caused by the direct slurry impact, the probe is a wear item. Probe life is related to particle hardness and size, which is

obviously finer in the overflow stream compared to the feed stream. Currently the software provides up to five reference mesh sizes to be incorporated into a process control strategy. Once installed on the battery, the PST system is calibrated empirically over a range of particle sizes determined by the client. The detection of abnormal cyclones as discussed in this paper can involve PST measurements above the maximum size of the calibrated range, thus the detection of abnormal events improves as the maximum calibration size increase. Figure 2 shows the main components of the PST system.

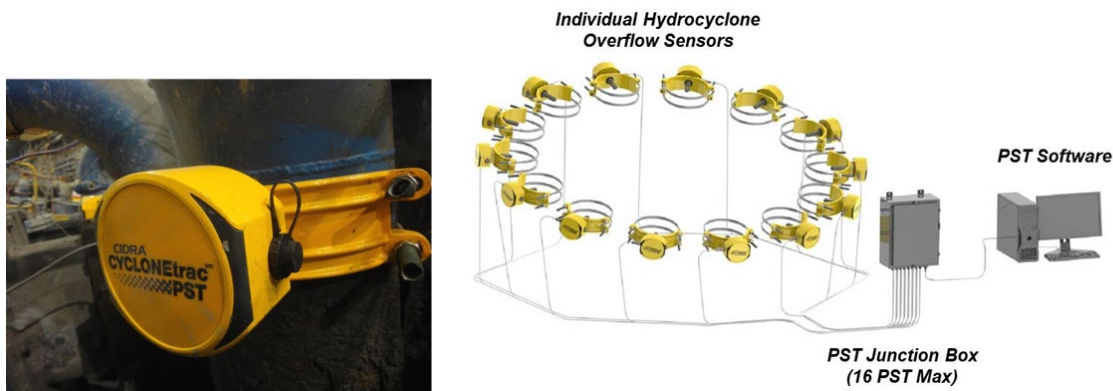


Figure 2 PST mounted sensor head (left), and system with interconnections (right)

## PLUGGED CYCLONE SIMULATION

To assess the impact of an abnormal cyclone on the overall grinding line performance, a typical Population Balance Model (PBM), size-by-size ball mill / classification circuit simulator, was developed using the EXCEL based, J-Tools software (Figure 3) where the abnormal cyclone is labeled '12' and the normal cyclones in the same cluster are labeled '11'.

The key underlying assumption for the purpose of developing the simulator is that, in a properly designed hydrocyclone cluster distributor, the feed pressure to every cyclone (including any plugged cyclones) would be the same for every individual cyclone, as well as the density (% Solids) of the slurry being fed to each of them. Under these assumed conditions, the resulting volumetric flowrate (m<sup>3</sup>/h) to each cyclone will be in direct proportion to the sum of their apex and vortex discharge areas (i. e.,  $\pi DU^2/4$  and  $\pi DO^2/4$ , respectively); hence, all other dimensions the same, the relative volumetric feed ratio ( $\Phi$ ) between a normally operating cyclone ( $Q_N$ ) and a fully/partly plugged cyclone ( $Q_P$ ) would be given by:

$$\phi = Q_P/Q_N = (DU_P^2 + DO_P^2)/(DU_N^2 + DO_N^2) \quad (1)$$

where the sub-index N denotes a normally operating cyclone and P denotes a cyclone with a fully/partly plugged underflow discharge (i. e.,  $DU_P$  approaching zero).

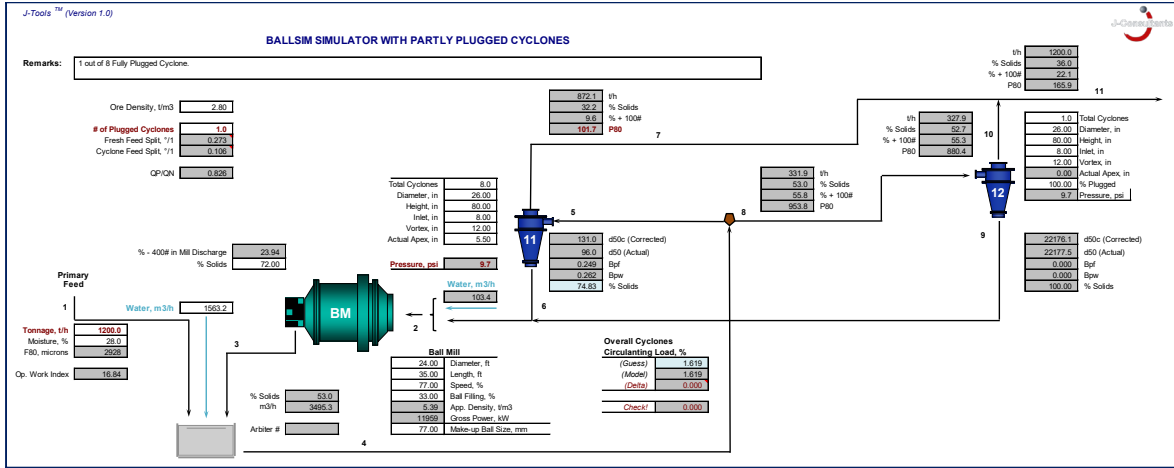


Figure 3 J-Tools simulation of a fully/partly plugged hydrocyclone

Considering that all cyclones have the same characteristic dimensions ( $DO_P \equiv DO_N$ , in particular), the relative volumetric feed ratio ( $\phi$ ) between a normally operating cyclone ( $Q_N$ ) and a fully/partly plugged cyclones ( $Q_P$ ) would be given by:

$$\phi = Q_P/Q_N = [1 + (DU_P/DO_N)^2]/[(1 + (DU_N/DO_N)^2)] \tag{2}$$

For mass balance compliance around the classifiers, the total feed flowrate to the complete cluster of cyclones, ( $Q$ ), is given by:

$$Q = N_P Q_P + (N - N_P) Q_N \tag{3}$$

where  $N$  is the total number of cyclones in the cluster. Solving for the total flow split ( $N_P Q_P/Q$ ) absorbed by the plugged cyclones:

$$N_P Q_P/Q = 1/(1 + (N/N_P - 1) / \phi) \quad \text{for } N_P > 0 \tag{4}$$

From Equation 4, it is then possible to estimate the proportion of the total cyclone cluster feed into plugged cyclones ( $N_P Q_P/Q$ ). It is convenient to express the degree of apex plugging (% Plugged) in terms of its partly plugged apex dimension ( $DU_P$ ) in comparison to the normally operating apex dimension ( $DU_N$ ):

$$\% \text{ Plugged} = [1 - (DU_P/DO_N)^2] * 100 \tag{5}$$

equivalent to:

$$DU_P = DO_N [1 - (\% \text{ Plugged}/100)^{0.5}] \tag{6}$$

Different degrees of abnormal behaviour for cyclone '12' can be created by varying its apex area from its nominal unconstrained value (0% Plugged) to approximately zero (100% Plugged), thus deflecting an increasing proportion of its feed slurry up to the coarsening overflow stream.

As shown in Figure 3, the total cyclone feed flowrate (stream #4) is split at a hypothetical node (orange pentagon) with one part (stream #5) directed to the normally operating cyclones, and the remaining part (stream #8) directed to cyclone '12'. The overflow stream from the abnormal cyclone (stream #10) joins with the overflow stream from the normal cyclones (stream #7) to form the final consolidated overflow (stream #11) that goes to flotation. The underflow from the abnormal cyclone (stream #9) joins with the underflow stream from the normal cyclones (stream #6) to be returned to

the ball mill. The user can then specify the number of plugged cyclones desired, normally just one cyclone at a time.

Figure 4 summarizes the projected results for an 8-cyclone cluster example operating at five different plugging conditions ranging from all 8 cyclones normal and 1 of 8 partly plugged in the 25% to 100% range.

	% Plugged					
	0	25	50	75	100	
<b>Fresh Tonnage Split, °/1</b>						
Abnormal Cyclones	0.125	0.180	0.199	0.222	0.273	↑
Normal Cyclones	0.875	0.820	0.801	0.778	0.727	↓
<b>Cyclone Feed Flowrate Split, °/1</b>						
Abnormal Cyclones	0.125	0.111	0.107	0.106	0.106	↓
Normal Cyclones	0.875	0.889	0.893	0.894	0.894	↑
<b>Cyclone Feed Flowrate, m<sup>3</sup>/h/Cyclone</b>						
Abnormal Cyclones	522	443	428	420	413	↓
Normal Cyclones	522	509	508	506	499	↓
<b>Operating Conditions</b>						
Circulating Load, °/1	2.06	1.88	1.83	1.77	1.62	↓
Op. Work Index, kWh/t	15.28	15.44	15.63	15.89	16.84	↑
<b>Normal Cyclone O'Flow</b>						
t/h	1050	984	961	933	872	↓
Cyclone Pressure, psi	10.35	9.97	9.94	9.88	9.70	↓
<b>P80</b>	<b>143</b>	<b>134</b>	<b>126</b>	<b>118</b>	<b>102</b>	↓
% +100#	18.40	16.48	14.91	13.18	9.64	↓
<b>Plugged Cyclone O'Flow</b>						
t/h	150	216	239	267	328	↑
Cyclone Pressure, psi	10.35	9.97	9.94	9.88	9.70	↓
<b>P80</b>	<b>143</b>	<b>195</b>	<b>246</b>	<b>322</b>	<b>880</b>	↑
% +100#	18.40	30.20	38.28	45.11	55.27	↑
<b>Combined Cyclone O'Flow</b>						
t/h	1200	1200	1200	1200	1200	
<b>P80</b>	<b>143</b>	<b>145</b>	<b>148</b>	<b>152</b>	<b>166</b>	↑
% +100#	18.40	18.95	19.57	20.27	22.11	↑
<b>% Recovery</b>	<b>90.22</b>	<b>90.03</b>	<b>89.18</b>	<b>87.48</b>	<b>82.82</b>	↓↓

**Figure 4** Example of J-Tools simulations for the case of an 8-cyclone cluster where 1 of the cyclones is subject to various degrees of apex plugging, from 0 to 100%.

The first significant impact of an abnormal cyclone can be seen in the change in the fresh tonnage split, i.e. the ratio of the fresh tonnage exiting through the abnormal cyclone overflow to the total fresh tonnage being fed to the circuit. For the case of all 8 cyclones operating normally, the split is 0.125 as expected, i.e. the tonnage is split evenly between all cyclones. However, the split increases up to 0.273 as the degree of plugging is increased from 0% to 100%; that is, an increasing proportion of the fresh feed tonnage is being delivered as a much coarser product through the fully plugged cyclone overflow. The plugged cyclone overflow delivers even more tonnage than the 0.104 fraction (0.894 / 7) being delivered by any of the individual normally operating cyclones.

Another significant effect of progressive plugging is the increase in coarseness of the overflow from the abnormal cyclone as measured by the P80 and the related measurement of % +100#. The P80

shows a dramatic increase from the normal 143 µm to a maximum of 880 µm when the cyclone is 100% blocked. At the same time, the overflow of the normal cyclones becomes finer at 102 µm, in line with the actual response observed in the plant example shown in Figure 1. Finally, the effect of combining these very coarse and slightly finer flows into the combined cyclone overflow is to increase the P80 of this combined flow from the normal 143 micron to a maximum of 166 micron. This increase in P80 may not appear too significant. However, if this is the only measurement that is available, as may be the case in most plants, then this may not even be considered worthy of corrective action. Or if action is taken, it could be the wrong action, with the operator or control system reducing the fresh feed because of the slight unwanted coarsening of the overall P80 that was detected, possibly being mistakenly attributed to the sudden introduction of harder ore. Meanwhile, the real problem is a plugged cyclone that has gone undetected.

### IMPACT ON FLOTATION RECOVERY

The very significant impact on the downstream flotation recovery of the valuable metal (say, copper) resulting from an abnormally operating cyclone can also be analysed using the developed J-Tools simulator. A convenient, size-by-size description of the flotation recovery process equation is provided by the fairly simple expression:

$$R_i = R_{max} [ \exp (-0.693 (d_i^* / d_{crit}^C)^{m_C} - \exp (-0.693 (d_i^* / d_{crit}^F)^{m_F} ) ] \quad (7)$$

where:

- $R_i$  = Average recovery for particles in the size fraction  $d_i$  to  $d_{i+1}$
- $R_{max}$  = Maximum achievable recovery for any particle size in the flotation feed stream
- $d_i$  = Average particle size for the size fraction  $d_i$  to  $d_{i+1}$
- $d_{crit}^C$  = Critical size above which coarser particles start to float at decreasing recoveries
- $d_{crit}^F$  = Critical size below which finer particles start to float at decreasing recoveries
- $m_C, m_F$  = Shape factors (higher values reflect higher recovery sensitivity to particle size changes)

Figure 5 presents an example of this type of representation for characteristic parameters  $R_{max} = 96\%$ ,  $d_{crit}^C = 250 \mu\text{m}$ ,  $d_{crit}^F = 11 \mu\text{m}$  and shape parameters  $m_C = 2.5$  and  $m_F = 4.0$ , showing a significant decrease in recovery for particles coarser than 250 µm and a slight decrease for particles finer than 11 µm, as it is characteristic of conventional flotation applications.

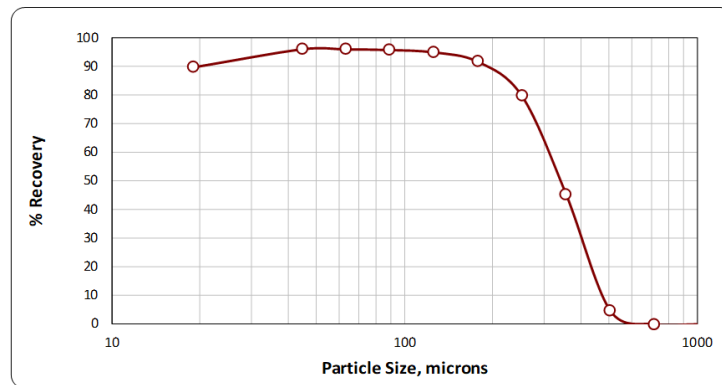


Figure 5 Example of size-by-size recovery

The combination of the size-by-size recovery values with the size-by-size overall cyclone overflow PSD predicted by the simulator gave rise to the overall valuable recovery values already presented at the bottom of Figure 4. The true costly effect of the fully blocked cyclone is revealed in the decrease in recovery from a normal 90.22% to a much lower 82.82% when the abnormal cyclone is 100% blocked. The reason is clearly shown in Figure 6 where the overflow PSD's for the normal cyclones and the fully plugged cyclone are shown together with the flotation recovery curve. When all cyclones are operating normally, 95% of the particles in the overflow are finer than the critical flotation size of 250  $\mu\text{m}$  (the size above which recovery drops dramatically). When one cyclone becomes fully plugged, a slightly higher 98% of the particles in the overflow from the non-plugged cyclones are finer than 250  $\mu\text{m}$  and within the floatable size range, but they now represent only 73% of the total tonnage being ground. The remaining 27% of the total tonnage is discharged from the plugged cyclone where only 59% of its particles are finer than 250  $\mu\text{m}$  and thus able to float. In summary, if one of eight cyclones is blocked, its fresh tonnage processed has increased by 2X, from 12.5% to 27.3%, but the amount of floatable material being discharged has decreased from 95% to 59%. The net effect being the decrease in overall recovery of approximately 7.4%.

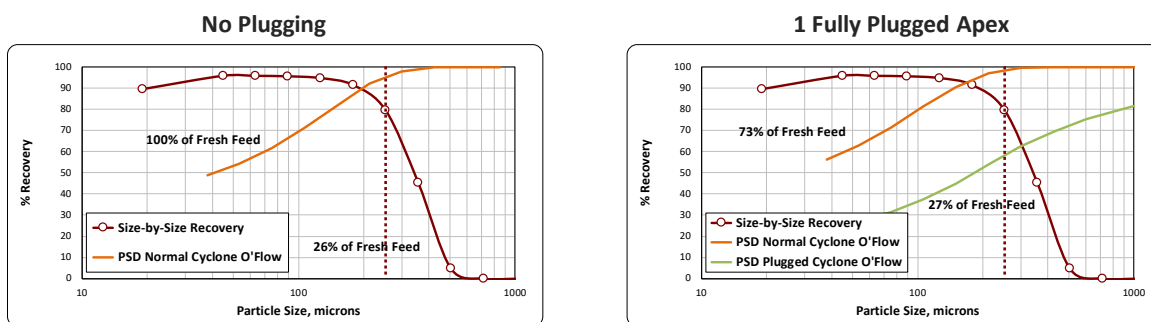


Figure 6. Typical flotation recovery curve and overflow particle size distribution curves for two cases: no plugged cyclones with 100% of fresh feed being properly classified (left); and one fully plugged cyclone with 27% of the fresh feed not being classified and the remaining 73% being slightly finer (right).

## OUTLIER DETECTION ALGORITHM

PST signals from normally operating cyclones in a battery, operating in a steady-state condition for a defined period of time, as those shown in the left half of Figure 1 above, will typically exhibit natural random fluctuations ( $Y_i$ ) normally distributed around a given mean value ( $Y_{AVE}$ ) with a characteristic standard deviation ( $\sigma$ ). When a cyclone becomes partially or fully plugged its PST signal differs significantly from the others and can be considered a statistical “outlier”. The Grubbs Test (Grubbs, 1950; Grubbs, 1969) is a well-known statistical criterion for the detection of “outliers” or “out of range” values with respect to a series of other comparable values in a given time series, and it is hereby proposed to be adopted for the on-line analysis of PST signals.

### Grubbs Outlier Detection Test

For statistical data analysis, the Grubbs Test, also known as the maximum normalized residual test or extreme studentized deviate test, is a statistical criterion used to detect outliers in a univariate data set assumed to come from a normally distributed population. The Grubbs test statistic is defined as:

$$G = (Y_{MAX} - Y_{AVE}) / \sigma \quad (\text{one-sided}) \quad (8)$$

Where  $Y_{MAX}$  is the largest value of a set of  $N$  random observations ( $Y_i$ ,  $i = 1, N$ ),  $Y_{AVE}$  is the average of all those values and  $\sigma$  is their standard deviation. This way,  $G$  denotes the largest standard deviation from the mean in units of  $\sigma$ .

In a one-sided test,  $Y_{MAX}$  is to be rejected as an outlier, at a significance level  $\alpha$ , if

$$G = (Y_{MAX} - Y_{AVE}) / \sigma > (N - 1) t^2 / N^{0.5} / (N - 2 + t^2)^{0.5} \quad (9)$$

with  $t$  denoting the upper critical value of the t-distribution with  $N-2$  degrees of freedom and a significance level of  $\alpha/N$ .

The following four Cases provide examples of Grubbs Test application to the processing and interpretation of PST signals from a conventional 8-cyclone cluster, based on randomly generated data via a Monte Carlo simulation technique.

### Case 1 – Plugged Cyclone Detection

As shown in Figure 7, after 10 minutes of normal operation, Cyclone 1 goes into a fully plugged condition, producing a much coarser overflow, while the other 7 cyclones start producing a somewhat finer overflow, in line with the actual data trends shown in Figure 1 as well as anticipated by the J-Tools simulator discussed above. Due to the uneven circuit mass flowrate distribution in favor of the plugged cyclone, the latter predominates and the overall cyclone overflow stream (normal + plugged cyclones) goes slightly coarser (red trace in Figure 7). Important to note that this change would very likely go undetected if only the combined overflow were being measured and controlled and not every individual cyclone overflow. Due to the availability of the individual cyclone PST signals, the application of the described on-line Grubbs Test promptly detects this event (upper chart in Figure 7) and would suggest the immediate replacement of the abnormal cyclone with another idle cyclone available in the cluster (*Note: if any given cluster was designed to operate with 8 cyclones, it should be equipped with at least 10 cyclones in total, so there should always be idle cyclones available to replace plugged cyclones*). Interestingly, if in fact the slightly coarser combined overflow product were to be detected by a control system, it would most likely take the

costly action of reducing the circuit fresh feed tonnage because it would have determined that the current feed rate was too high for the circuit to grind to the desired product size, e.g. due to an increase in ore hardness.

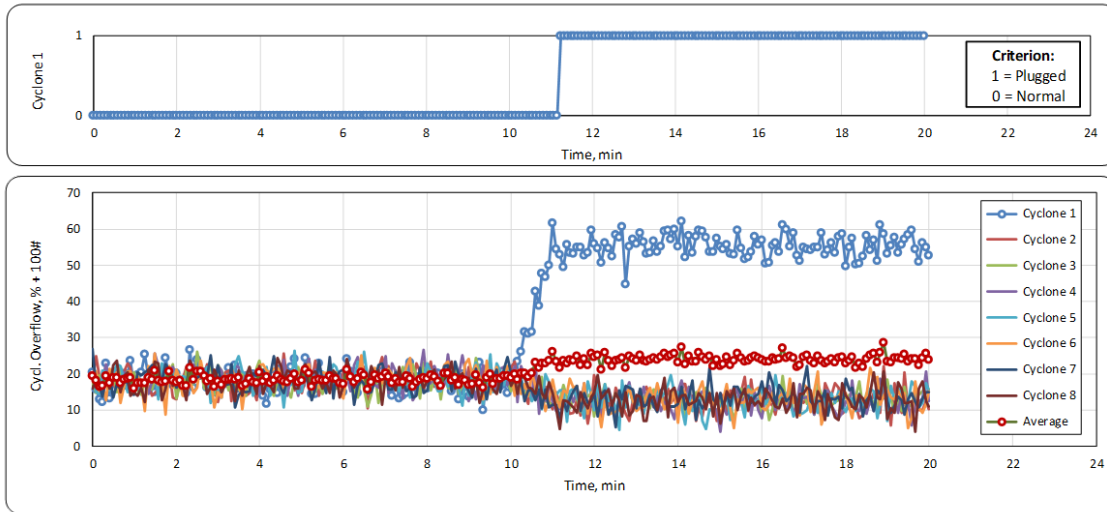


Figure 7. Example of plugged cyclone detection via on-line application of the Grubbs Test outlier detection criterion.

### Case 2 – Overall Coarser Grind

Contrary to other cyclone open/close algorithms (typically based on fixed control bands) when all cyclones go coarser, as shown in Figure 8, as a result of changing operating conditions, the Grubbs Test correctly does not highlight any candidate cyclones for replacement (see upper chart in Figure 8); thus avoiding repetitive over-reaction of the control system when such situations are present during normal operation.

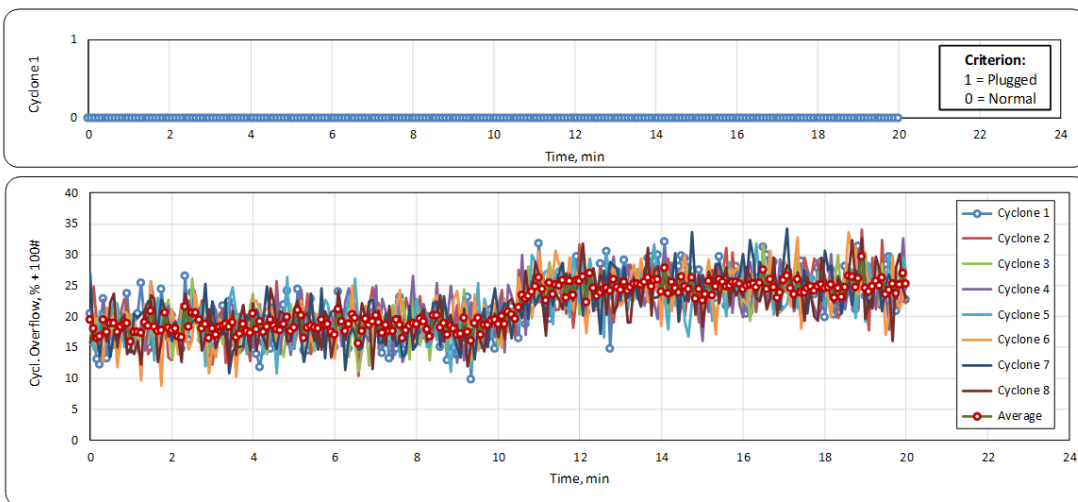
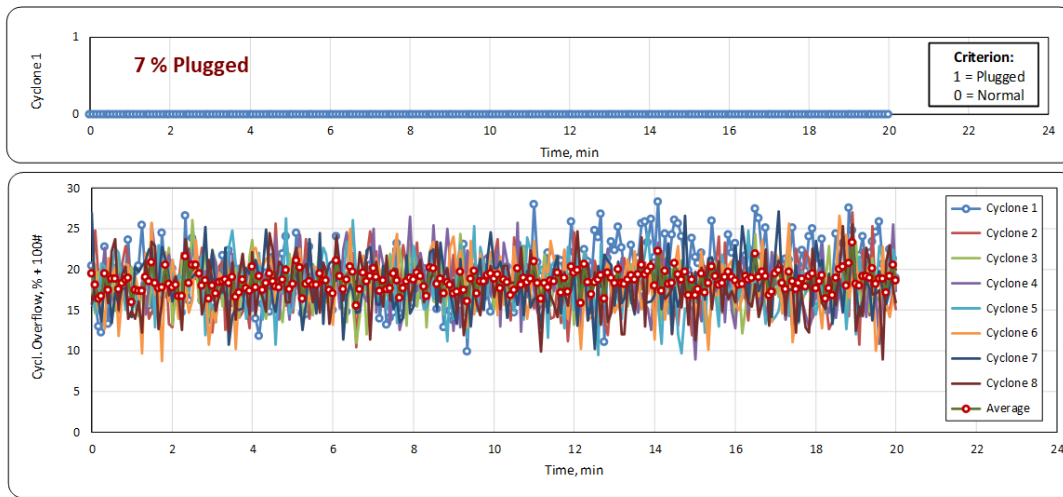


Figure 8. Example of the Grubbs Test outlier detection criterion demonstrating insensitivity to overall coarsening of the grind size; that is, no plugging.

### Case 3 – Algorithm Detection Limit

In any application, the detection limits may be adjusted to a preferred range by properly specifying the statistical parameters of the algorithm, such as the significance level  $\alpha$  or the number of random observations  $N$  as defined in the Grubbs Test. In the example shown in Figure 9, the abnormal cyclone detection algorithm can highlight emergent apex plugging events as early as 7-10% plugging. The actual detection limit will depend on various factors unique to each application, and the calibrated range of the PST system.



**Figure 9.** Example of Cyclone 1 just below the threshold of its detection range of 7-10% plugging.

#### Case 4 – Application to Actual Data

For the actual case example presented earlier in Figure 1, it may be also shown that the proposed outlier detection algorithm would have clearly detected the abnormal Cyclone 9 response as shown in 10.

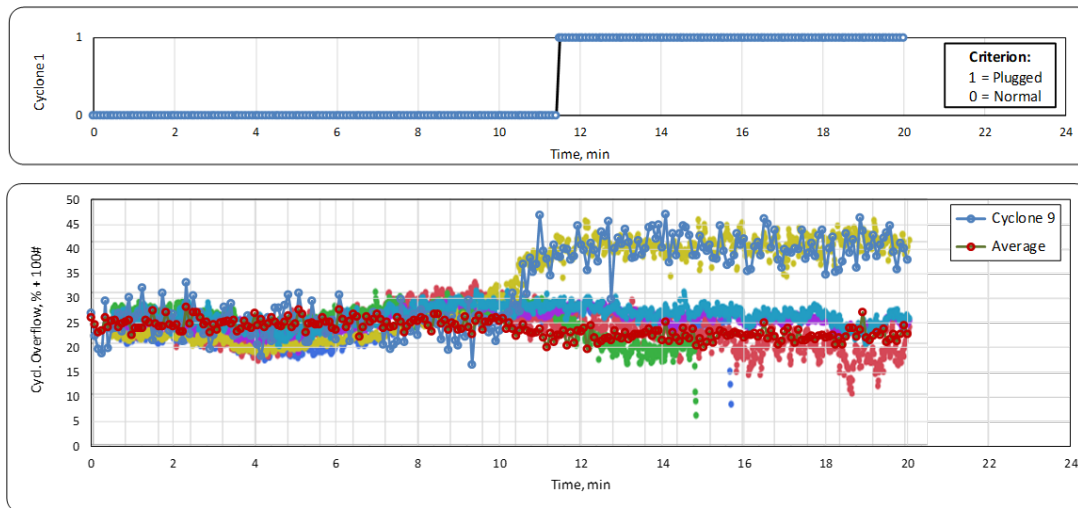


**Figure 10.** Example of the outlier detection algorithm detecting the abnormal Cyclone 9 in the example case shown in Figure 1.

### INTEGRAL CONTROL STRATEGY

Proper on-line utilization of the proposed outlier detection algorithm allows for the effective implementation of a novel integral control strategy for the whole production line (i.e. SAG or HPGR, Ball Milling and Flotation).

Focusing on the ball milling stage, following the schematic representation of the proposed expert control logics in Figure 11, the first step in the control cycle is to confirm if the circuit overflow P80 (or some reference mesh size) is compliant with established acceptable range. If P80 is too fine or within range, no further action is required and control is transferred back to the upstream grinding stage (in this example, the SAG mill). Contrarily, if P80 is too coarse, the next step is to apply the Grubbs Test to identify any possible plugged cyclones. If positive, the plugged cyclone(s) should be promptly replaced with other idle cyclone(s) in the cluster. If negative, various grinding circuit conditions, such as cyclone pressure, mill power, circulating load, are examined and adjusted whenever required. If no adjustments are found to be possible or necessary, then the P80 contingency is declared to be caused by the upstream SAG mill delivering too much flow (for the current ore hardness) to the ball mills and the control is transferred back to the SAG mill under RESTRICTED Mode.

Clearly, this optimizing control strategy is only made possible thanks to the availability of PST on-line size measurements for every individual cyclone in the cluster.

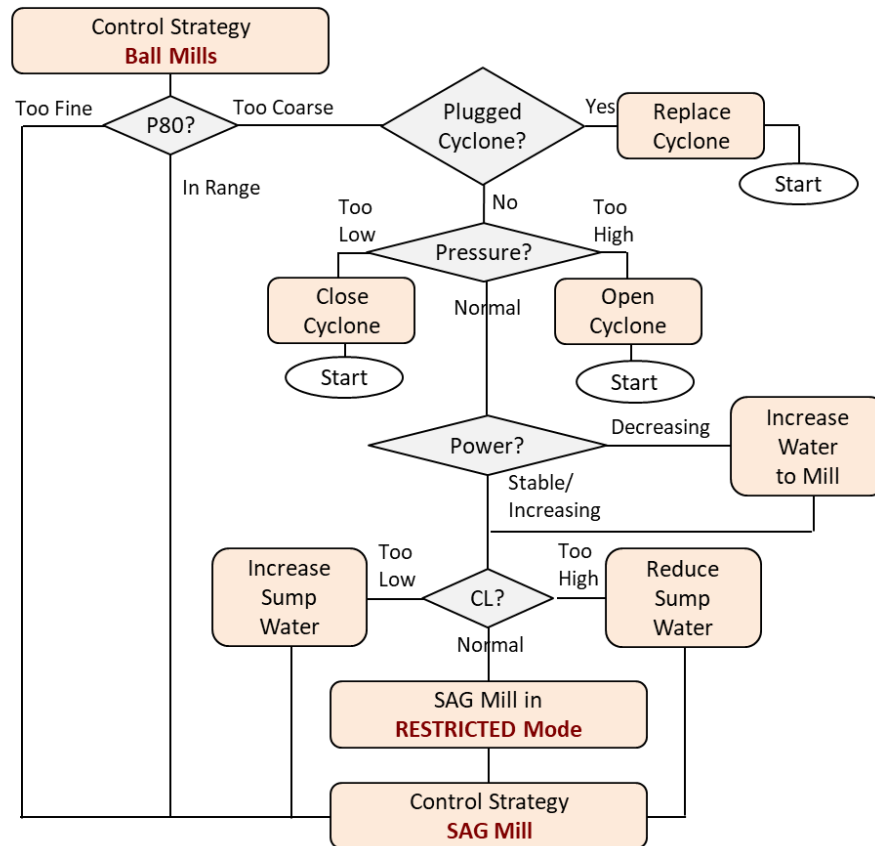


Figure 11 Schematics of the proposed Expert Control Logics for the ball milling stage.

## FINAL REMARKS

For decades the absence of reliable real-time on-line particle size measurement has limited the implementation of automatic particle size control strategies that might allow concentrators to maximize valuable metal production. By measuring the particle size on the overflow of every cyclone, it has been shown that CiDRA’s PST system enables the detection and control of individual abnormal cyclones, going much beyond the traditional battery-level control. The proposed Expert Control Strategy would not be feasible with alternative near-line particle size measurement devices, limited to process just the combined overflow from all cyclones in the cluster at measurement frequencies much lower than those required for effective control strategies.

The condition of an abnormal cyclone has been simulated by progressively reducing the apex diameter to simulate partially to fully-plugged cyclones. This simulation enables an in-depth quantitative understanding of the event and the significant effect a single abnormal cyclone can have on an entire cyclone cluster.

For the particular 8-cyclone cluster example here discussed, the simulations reveal that for a fully blocked cyclone, a disproportionately large 27% of the total tonnage being ground exits the overflow of the plugged cyclone of which only 60% is floatable at acceptable recovery levels, resulting in an estimated 7-8% loss in valuable metal.

By applying a statistical outlier detection algorithm, such as the described Grubbs Test, it is possible to detect an “outlier” or “out of range” value (such as the PST signal from an abnormal cyclone) with respect to a series of other comparable values (such as the PST signals from normally operating cyclones). Contrary to other cyclone open/close algorithms, it does not highlight abnormal cyclones for replacement when all cyclones change their product size simultaneously due to an operating condition change, such as when all cyclone produce coarser overflows. The detection limit can be adjusted by properly specifying the statistical parameters of the algorithm.

## REFERENCES

- Grubbs, F.E., (1950), “Sample Criteria for Testing Outlying Observations”, *Annals of Mathematical Statistics*, 21 (1): 27-58.
- Grubbs, F.E., (1969) ‘Procedures for Detecting Outlying Observations in Samples’, *Technometrics*, Vol. 11, No. 1, *Published by American Statistical Association and American Society for Quality*, viewed 06 November 2019. <http://webspaceship.edu/pgmarr/Geo441/Readings/Grubbs%201969%20-%20Detecting%20outlying%20observations%20in%20samples.pdf>
- Maron, R., O’Keefe, C., Sepúlveda, J.E. (2017) ‘Assessing the Benefits of Automatic Grinding control Using PST Technology for True On-Line Particle Size Measurement’, *Proceedings of PROCEMIN 2017 13<sup>th</sup> International Mineral Processing Conference, Santiago, Chile*.
- Maron, R., Sepulveda, J.E., Jordens, A., O’Keefe, C., Walqui, H. (2019) ‘Coarser Grinding: Economic Benefits and Enabling Technologies’, *Proceedings of MINEXCELLENCE 2019, 4<sup>th</sup> International Seminar on Operational Excellence in Mining, Santiago, Chile*.